X-ray Emission Processes in Radio Jets

D. E. Harris,
Smithsonian Astrophysical Observatory, 60 Garden St. Cambridge, MA 02138
and

H. Krawczynski,
Yale University, New Haven, CT

ABSTRACT

The emission processes responsible for the observed X-rays from radio jets are commonly believed to be non-thermal, but in any particular case, it is unclear if synchrotron emission or one or more varieties of inverse Compton emission predominates. We present a formulation of inverse Compton emission from a relativistically moving jet ("IC/beaming") which relies on radio emitting synchrotron sources for which the energy densities in particles and fields are comparable. We include the non-isotropic nature of inverse Compton scattering of the relativistic electrons on photons of the cosmic microwave background (CMB) and provide beaming parameters for a number of jets. A list of X-ray emitting jets is given and the jets are classified on the basis of their morphology and spectral energy distribution to determine their likely emission process. We conclude that these jets have significant bulk relativistic velocities on kpc scales; that higher redshift sources require less beaming because the energy density of the CMB is significantly greater than locally; and that for some nearby sources, synchrotron X-ray emission predominates because the jet makes a large angle to the line of sight.

Subject headings: galaxies: jets—magnetic fields—radiation mechanisms: non-thermal

1. Introduction

X-ray emission associated with radio jets in extragalactic sources now comes in a large variety of diverse characteristics. When this sort of emission was first isolated (e.g. the radio galaxy M87 with the EINSTEIN OBSERVATORY, Schreier, Gorenstein, & Feigelson 1982) and there were only a few examples, it was tempting to work on the assumption that the emission process was definable and would apply to all examples. This notion persisted into the ROSAT era until a convincing case was made that the terminal hotspots of Cygnus A represented synchrotron self-Compton (SSC) emission (Harris, Carilli, & Perley, 1994).

With the advent of the CHANDRA OBSERVATORY, the number of sources has almost tripled (from 7 to at least 19) yet there remain substantial problems in determining the emission process responsible for the X-rays in some sources. Although broken power laws connecting the radio, optical, and X-ray data are still viable spectral models for a few sources, a number of other sources are observed to have such a low flux density in the optical that the indicated cutoff in the spectrum would preclude a simple connection to the X-ray data.

The introduction of the 'beaming model' (Tavecchio et al. 2000, Celotti et al. 2001) in the particular case of PKS0637 was presented as an escape from this dilemma. In this model, the enhancement of the X-ray emission relative to the synchrotron (radio/optical) is explained by hypothesizing a bulk velocity of the jet fluid which is relativistic even on large (kpc) scales. If this were the case, in the frame of the jet the effective photon energy density of the cosmic microwave background (CMB) would be augmented by the square of the jet's Lorentz factor, Γ, and it was

demonstrated that quite reasonable combinations of Γ and the beaming factor, δ could be invoked to explain the observed intensities.

In this paper we review the common emission processes (section 2); present a current list of jet sources and suggest a classification scheme (section 3); describe a formulation of the beaming model which relies on an evaluation of the magnetic field strength from the equipartition field and includes the anisotropic nature of the IC scattering (section 4); and examine the conflicting evidence and ramifications for the synchrotron and inverse-Compton (IC) models (section 5). The appendix contains the details of our beaming formulation.

For numerical results we use cgs units unless stated otherwise and assume H_0=50 km s^{-1} Mpc^{-1}; and q_0=0. We follow the convention that the spectral index of a power law is defined by flux density, $S_\nu = k\,\nu^{-\alpha}$.

2. Overview of emission processes

2.1. Thermal bremsstrahlung

For many sources which display convincing evidence that the X-ray and radio emission originate in the same volume, (e.g. hotspot B of 3C390.3, Harris Leighly & Leahy 1998) it has been argued that thermal bremsstrahlung does not provide a satisfactory model for the X-ray emission because the required amount of hot gas is large ($\approx 10^{10} M_\odot$), over-pressured, far from the parent galaxy, and the predicted Faraday rotation and depolarization are not observed. Recent Chandra results (e.g. 3C 273, Marshall et al. 2001a) confirm that the X-ray emission from jet features has no line emission and is best characterized by a power law.

2.2. Synchrotron emission

Synchrotron emission has been considered the 'process of choice' for X-rays from knots in radio jets mainly because the optical polarization observed in sources such as M87 is convincing evidence that the optical emission as well as the radio emission comes from the synchrotron process. Demonstrations that the X-ray intensity was consistent either with a single power law extrapolation from radio and optical bands (e.g. hotspot B of 3C 390.3, Harris, Leighly, & Leahy 1998) or with a broken power law (e.g. knot A in M87, Biretta, Stern, & Harris 1991) were taken as circumstantial evidence that the X-rays were also generated by synchrotron emission. Required for this model is the presence of electrons with Lorentz factor $\gamma > 10^7$ (cf. values of 10^5 for optical emission). In the typical equipartition fields of B $\approx 10^{-4}$G, the radiation half lives τ_o of the X-ray emitting electrons would be of order 10 years (however, see Aharonian (2001) for problems associated with very fast cooling times).

There are, however, a number of sources for which the optical flux densities or limits preclude a simple construction of a broken power law. In general, assuming the usual shock acceleration processes and dominance of losses to the relativistic electrons that go with the energy squared, we expect that both the electron distribution and the resulting synchrotron emission spectrum will be concave downward when displayed on the usual log S_ν vs. log ν plot. For this reason, X-ray intensities that lie well above the extrapolation of the radio/optical synchrotron spectrum are taken to be strong evidence against the 'simple' synchrotron model.

The emission of most of these sources however can still be explained with inhomogeneous synchrotron models. Spatially separated emission components which cannot be resolved with the current X-ray detectors would be the consequence of diffusive shock acceleration with a time dependent high energy cut-off of accelerated particles. While the low energy radio and optical emission is dominated by radiatively aged particle populations further downstream, the X-ray emission is only emitted by recently accelerated particles. In this scenario the projected extension of the X-ray emission region is either given by the projected size of the accelerating shock, or by the distance the downstream plasma travels before the highest energy electrons cool away. For 3C 120 such an interpretation encounters the difficulty that the optical to X-ray energy spectrum is as hard as $\alpha_{\rm OX}$ <0.35 which indicates a spectrum of accelerated particles with a spectral index, $p \lesssim 1.7$ (even in the optimistic case that the X-ray electrons did not cool substantially); harder than the canonical values of 2 expected for acceleration at strong non-relativistic shocks.

Another class of models involves high energy

protons. These models and their difficulties are described in Mannheim, Krulls, & Biermann (1991) and Aharonian (2001).

2.3. Inverse Compton emission

Inverse Compton emission has a distinct advantage over X-ray synchrotron emission in that extremely high energies for the emitting electrons are not required. What is required are both enough electrons and enough energy density in photons of the proper energy to produce the desired scattered photons: $\nu_{out} \approx \nu_{in} \times \gamma^2$.

2.3.1. Synchrotron self Compton emission

Unlike synchrotron emission for which the radio data often provide no clear indication about the higher energy parts of the electron spectrum, accurate predictions of source intensity can be calculated for SSC emission. Given a reasonable estimate for the emitting volume, it is possible to calculate the photon energy density from the synchrotron spectrum and then determine what B field is required to have the right number of electrons to give the observed (radio) synchrotron and the observed (X-ray) IC emissions.

Although SSC emission is mandatory for all synchrotron sources, it is usually the case that the photon energy density (u_ν) is significantly smaller (i.e. by factors of 100 or more) than the energy density of the magnetic field (u_B) and thus the major energy loss for all electrons is via synchrotron emission (and the SSC component is too weak to observe or distinguish from other emissions).

There are however, four FRII radio galaxies with convincing SSC X-ray emission from their (terminal) hotspots: Cyg A (Harris et al. 1994; Wilson,, Young, and Shopbell 2001a); 3C 295 (Harris et al. 2000); 3C 123 (Hardcastle, Birkinshaw, & Worrall 2001a), and 3C 263 (Hardcastle et al. in preparation). For all of these sources, predicted SSC emission was calculated from the radio data, proposals were written, and the hotspots were detected as predicted. In all cases, the average magnetic field strengths derived from the SSC equations are consistent with equipartition fields for the case of little or no contribution to the particle energy density from relativistic protons. The hotspots of these sources are, so far, the only resolved structures for which convincing SSC models have been published.

2.3.2. IC emission from the microwave background

Except for high redshift sources, IC emission from the relativistic electrons scattering off the CMB is incapable of producing the observed intensity of X-rays unless the beaming model is invoked with relativistic values of the bulk jet velocity (see section 4). The beaming model is attractive because most or all of the X-ray emitting jets are one sided and the model permits the relative increase of the effective photon energy density to that in the magnetic field, thereby boosting the emission in the IC channel relative to that in the synchrotron channel.

2.3.3. IC emission from other photons

External photons have been employed successfully in explaining X-ray emission from some radio lobes (Brunetti et al. 2001). However, it is unlikely to apply to knots far removed from the hypothesized highly luminous quasar-like core and Brunetti's model provides IC enhancement on the receding side of the source, not the approaching side as observed in our sample.

Celotti et al. (2001) discuss the possibility that emission from a high velocity 'spine' of a jet may serve as seed photons for IC emission from a lower velocity sheath. Generally, a wide latitude of inventiveness is allowed for IC emission since the dominant contribution to the photon energy density may be anisotropic and hence not directly observable.

3. Classification of sources

The contents of this section are 'subject to change' since much of our information is incomplete. The reason for including this source list is to provide an overview. Some aspects of the classification are subjective and we anticipate changes as new data become available. We maintain current information at http://hea-www.harvard.edu/XJET/.

Table 1 contains a list of bona fide X-ray jet sources known to us as of 2001 March. In the last column is the classification which is described here.

3.1. SSC

This category is perhaps more secure than the others because the data confirm the predictions rather well. All 4 SSC sources (sec. 2.3.1) are FRII radio galaxies and their terminal hotspots rather than brightness enhancements in the jets are the SSC emitters. For all of these, the magnetic field strengths in the hotspots are in the range 100 to 400 μG, values consistent with the equipartition field for the case of little or no contribution to the particle energy density from protons. Synchrotron luminosities and lifetimes are unaffected by the IC losses and the electrons responsible for the observed X-rays are those emitting synchrotron emission in the normal radio band. Alternative models for these hotspots are the generation of high energy electrons via the PIC (Proton Induced Cascade, Mannheim et al. 1991) or proton synchrotron (Aharonian 2001) processes, both of which would require much stronger magnetic fields ($B \gg 500\mu$G).

3.2. Synchrotron

Mindful of ongoing debate about the evidence for spectral cutoffs from optical data (sec. 2.2), we classify M87 knots D, A, and B as synchrotron emitters (Biretta, Stern, and Harris, 1991; Marshall et al., 2001b). Additional sources in this category are 3C 390.3 hotspot B (Harris et al. 1998), knots A1 and B1 in the 3C 273 jet (Marshall et al. 2001a), and 3C 66B (Hardcastle, Birkinshaw, & Worrall, 2001b) although for some of these, there is the problem that a cooling break in the emission spectrum has not been isolated.

The extension of the synchrotron spectrum from the optical to the X-ray has only a small effect on the total energy and on the calculation of the equipartition magnetic field. However, this model requires the extension of the electron spectrum from $\gamma \approx 10^5$ to $\geq 10^7$. The primary observable consequence is that the electrons responsible for the X-rays have lifetimes of order 10 to 100 years.

If a somewhat 'ad hoc' additional spectral component is allowed (sec. 5.2; i.e. a high energy component of the electron energy distribution with a flatter spectrum than that observed in the radio/optical domain), then synchrotron emission models can be devised for sources such as Pictor A (Wilson, Young, & Shopbell 2001b, section 4.2.2.2), 3C 273 knot D, PKS 0637, and 3C 120 (Harris et al. 1999; where a very hard spectral index of accelerated particles of p=1.7 would be required). The SSC sources (sec. 2.3.1) could also be accomodated by synchrotron models if additional spectral components are allowed.

3.3. Bulk relativistic velocities

In sections 4 and 5 we discuss many of the details and ramifications of this model. While there is little debate concerning the utility of the beaming model in its ability to explain a larger ratio of X-ray to synchrotron emission than other models, there is no completely convincing evidence that kpc-scale jets actually have bulk velocities close to c.

Beaming models have been presented for PKS0637 (Celotti et al, 2001; Tavecchio et al. 2000) and for 3C 273 (Sambruna et al. 2001). For the knots in these jets, viewing angles are generally required to be less than 10°, Γ values range from 5 to 20, and equipartition fields are significantly smaller than for unbeamed synchrotron emission. A very significant difference between beaming and synchrotron models is that the beaming model posits that the electrons responsible for the observed X-rays are at the very bottom of the electron distribution with γ in the range 20-150. This implies that no variability is expected in the X-ray intensity. Because there is a significant difference between the electron energies producing the X-rays and those that produce radio synchrotron emission observable from the Earth with sufficient resolution to measure accurate spectral indices, there is a large uncertainty in the expected spectral shape of the electron distribution at low energies, and consequently, in the predicted spectral shape and the intensity of the X-ray emission.

3.4. Discrepant radio/X-ray morphologies

Although most of the sources in Table 1 display spatial coincidence between the radio, X-ray, and optical morphologies, there are a few sources where this is not the case. Cen A, 3C 66B, and PKS 1127 are the three examples of this behavior in our collection. We do not believe that this effect results from limited angular resolution since it occurs in both the nearest (Cen A) and furthest

(PKS1127) source. In the case of Cen A, some offsets between the peak brightness of radio and X-ray are of order 2″ (34pc) while other features are coincident. For PKS1127, an offset of 0.8″ observed for knot B corresponds to 9 kpc.

For these jets, it is difficult to measure radio and x-ray intensities for well defined volumes. It is also the case that the PKS1127 jet is very weak in the radio (the source is a VLA calibrator) and the published radio data for Cen A do not have the combination of high resolution and s/n which are necessary for reliable inter-band comparisons. For 3C 66B and PKS1127, the peak X-ray brightness occurs upstream of the peak radio brightness. To obtain significant X-ray emission with little or no radio emission would require extreme beaming parameters or a distinct low energy electron population (sec. 5.2) for the beaming model or a flat high energy component of the electron spectrum for synchrotron models.

3.5. Not yet classified

Since data have not yet been published, we have not classified 3C 15, 3C 31, PKS0521, and NGC4261 in Table 1.

4. Determination of jet parameters within the beaming model

The beaming model introduced by Tavecchio et al. (2000) and Celotti et al. (2001) is appealing because it offers a method of increasing the IC emission relative to the synchrotron emission and because it was already clear from EINSTEIN and ROSAT results on M87, 3C 120, and 3C 390.3 that all known X-ray emitting jet features were one sided. Most of the new examples from Chandra detections maintain the one sided nature of X-ray emission, a natural consequence of the beaming model.

The following formulation is based on the assumption of equipartition in the synchrotron source in order to evaluate the magnetic field strength and accounts for the anisotropic nature of the IC emission in the jet frame. The details are given in the Appendix.

We define the constraints on the bulk relativistic flow velocity of the jet fluid, Γ; the viewing angle of the line of sight of the observer with respect to the jet velocity vector, $\theta_{\rm j}$; and the relativistic Doppler factor, δ. Once these constraints have been evaluated, we examine a number of source parameters:

- the segments of the electron energy spectrum responsible for both the synchrotron and IC emissions to make sure we end up with a self-consistent source model.
- the halflives of the various energy electrons.
- the basic parameters of the synchrotron source in the jet frame.

4.1. The case for equipartition

Over the years since its introduction (Burbidge, 1956), the concept of 'minimum energy' (or 'equipartition') has generated considerable debate and some confusion. Our view is that although it was originally borne of twin desperations (the staggering amount of non-thermal energy required for large synchrotron radio sources and the realization that it was almost impossible to disentangle the two primary parameters of synchrotron emission), a reasonable case can be advanced that most extragalactic synchrotron sources are not more than a factor of a few from having their average magnetic field energy density equal to the average energy density in relativistic particles: u(p) $\approx$ u(B).

Obviously we are unconcerned with the condition u(p) << u(B); it is the converse that has generated some interest as a means of increasing the relative emission in the IC channel compared to that in the synchrotron channel. For radio structures far from their parent galaxy it seems that the only mechanism which serves to maintain the integrity of a radio lobe is the magnetic field, acting as a boundary between the non-thermal plasma and the external thermal plasma. Direct evidence that some synchrotron emitting plasmas maintain their identity is provided both by the detection of cavities in cluster gas (Carilli, Perley, & Harris 1994) and by the observation that the B field direction is normally tangent to the edges of radio lobes (and not tangled as expected if turbulent mixing were occurring). If the particle energy density were much greater than u(B) it is unlikely that the field would confine the particles and radio sources would be transient phenomena without well defined boundaries.

Evidence for equipartition has come from the analyses of X-ray emission from terminal hotspots. In the study of Cygnus A hotspots, Harris et al. (1994) argued that if the observed X-ray emission were to be SSC emission, then the average magnetic field strengths (B_{IC}) would be very close to the equipartition fields estimated from the conditions: filling factor = 1 and no contribution to the particle energy density from relativistic protons. Since we have a fairly accurate estimate of the synchrotron photon energy density, we know that if there were more electrons than those corresponding to B_{eq}, we would over-produce the X-ray emission. Thus the derived value of B_{ic} is a firm lower limit and the only method of driving the hotspots out of equipartition with u(p) >> u(B) would be to add non-radiating particles. The three recent additions to the collection of resolved SSC emitters strengthen this evidence.

A number of additional arguments have been presented in favor of synchrotron sources being close to equipartition. Readhead (1994) used the observed distribution of brightness temperatures in support of equipartition but did not deal with the physical mechanism responsible. Bodo, Ghisellini & Trussoni (1992) refined earlier work by Syrovatskii (1969) and Singal (1986) on the effects of spiraling electrons and their associated diamagnetic moments and stated "The counter field produced by a cloud of relativistic electrons lead to an equilibrium between the magnetic field in the cloud and the energy density of radiating electrons."

Although it is possible to imagine synchrotron sources shortly after the introduction of a large amount of energy in particles, it is beyond the scope of this paper to consider the time scale required to return to equipartition. Since we are dealing with large (>kpc) scale structures, we believe that most of the emitting regions considered in this paper will be close to equipartition. However, questions are often raised such as "What is the extent of departure from equipartition for some given condition?" We note from equation A24 that a given change in Γ (which involves the same change in δ) will require a change in B(1) by this factor squared, and since u(B) goes as B^2, the change to u(B) goes as the fourth power. As an example, consider the beaming required for 3C120: Γ=39 (Table 2). How far from equipartition would we have to go to get Γ=10? The answer is of order 230 times less energy in the magnetic field than in particles. Although this calculation is approximate, the formulation presented in the appendices relies on the equipartition assumption only to evaluate the average field strength, and if some other estimate is available, it can be used in place of B'_{eq} in eq. A23.

4.2. Outline of the method

We first take the synchrotron spectrum from the observer's frame back to the jet frame. Since the beaming factor is unknown, this process is done (in principle) for trial values of δ. In the jet frame, we apply the usual synchrotron formulae (e.g. Pacholczyk, 1970) to solve for the equipartition field strength (eq. A6). Actually, the value of the average magnetic field for equipartition is inversely proportional to δ, so in practice, we need only calculate B'_{eq} for $\delta = 1$.

We then derive the expression for the IC emission (eq. A11) using the effective energy density of the CMB as seen by the jet fluid (eq. A13). We evaluate the quantity R (the ratio of IC to synchrotron luminosities) in two ways. First, we compute R from the integrated IC energy flux to the integrated synchrotron energy flux (eq. A21). This is done by converting observed synchrotron frequencies to electron energies (which involves the magnetic field strength) and integrating the IC emission from the same segment of the electron spectrum, taking into account the anisotropic radiation pattern of the IC component. Second, we compute the expected value of R from the ratio of the energy densities of the CMB to that in the magnetic field (both in the jet frame) (eq. A22). Equating these two expressions, we are able to solve for the beaming parameters which satisfy the equality (eq. A23). Since the jet parameters enter the R equations in rather complex ways because of the anisotropic nature of the IC emission, a numerical method is used. This is demonstrated in fig. 1 and we obtain a result consistent with that of Celotti et al. (2001) for PKS0637.

We use the following notation: we prime all quantities in the jet frame and, in cases where ambiguities could arise, we characterize jet parameters by the subscript "j" and electron parameters by the subscript "e".

4.3. Assumptions

- We assume that all the energy density of the CMB occurs at ν_{peak}, the peak of the black body distribution.
- We assume that in the jet frame equipartition holds between the energy densities of the relativistic particles and the magnetic field. This allows us to estimate the average field strength in the source. Moreover, we take the volume filling factor to be one and the contribution to the particle energy density by protons to be nil. If relativistic protons contribute significantly to the particle energy density, B_{eq} increases and beaming parameters become more extreme (larger values of Γ and smaller angles).
- The spectral index measured for the synchrotron spectrum at the lowest available frequencies continues unchanged to frequencies much lower that those accessible to Earth based telescopes. The gross attributes of this extrapolation must be consistent with radio emission arising from $\gamma'_e \approx 2000$ and X-ray emission (0.2-10 keV) arising from $25 < \gamma'_e < 300$. This extrapolation of the electron spectrum provides a large uncertainty in the beaming model and has been tacitly ignored by most previous formulations. At our current level of understanding, we do not have any convincing evidence on the amplitude or the power law index of the electron distribution at low energies.

4.4. Beaming parameters for a number of sources

In this section, we provide some of the key synchrotron parameters and beaming descriptors for a few knots in radio jets. For the synchrotron parameters, we use the standard expressions (e.g. Pacholczyk, 1970) with observables transformed back to the jet frame. For the beaming parameters, our solution to eq. A23 requires only 4 numbers:

- B(1), the equipartition field from the synchrotron model when δ=1 (no beaming)
- R(1), the ratio of amplitudes of the power law spectra: k_{ic}/k_{sync} where both amplitudes must refer to the same spectral index
- z, the redshift
- α, the spectral index

Table 2 gives the results and it can be seen that the beaming parameters range from quite modest values (e.g. PKS1127) to rather unbelievable extremes (3C 120). We have plotted the key results in fig. 2 which is a representation of the beaming parameters as a function of the observables (eq. A24).

5. Evaluation of beaming and synchrotron models

In this section, we deal with the conflicting evidence for general beaming models and for synchrotron models. On the one hand, some sort of beaming appears to be required by the observation that all of the known jet sources (excluding of course the SSC terminal hotspots) produce X-ray emission on only one side, and that is the side which has the only or dominant radio jet and for which relativistic effects have been demonstrated (usually on VLBI scales). On the other hand, for knots such as A1/3C273 or B/3C390.3, the observed X-ray intensity is accommodated by an extension of the power law connecting the radio and optical (i.e. the synchrotron spectrum). If the X-ray emission from these knots were to be IC/CMB emission enhanced by beaming, this situation would be only a coincidence.

5.1. X-ray spectra

In general, we expect synchrotron spectra to be concave downward when plotted on the usual log S vs. log ν plane. For high energy electrons, this is caused by the E^2 losses. Although we do not have reliable observational evidence on the shape or amplitude of the electron spectrum for $\gamma \leq 500$, our expectation is that the spectrum observed in the radio regime might flatten at lower frequencies, but it is unlikely to steepen. This view is dictated by the requirement to avoid divergences in the total number of electrons and integrated energy in the electron spectrum.

Reliable X-ray spectra are now available for only a few jets, but so far, the evidence is that the spectra are either the same as observed in

the radio/optical (e.g. 3C 273/A1, Marshall et al. 2001a), or steeper (α_x(M87)=1.5±0.4, Böhringer et al. 2001 and α_x(3C66B)≈ 1.3, Hardcastle et al. 2001b). This supports the synchrotron model and is not in accord with our expectation for beaming from low energy electrons. However, a relatively hard spectrum is found for PKS1127 (α_x=0.5±0.2; Siemiginowska et al. 2001), a jet that requires very modest beaming parameters. Similarly, Chartas et al. (2001) find α_x=0.85±0.1 for the outer jet in PKS0637, another likely beamed IC source. The X-ray spectral index may prove to be a key parameter in differentiating synchrotron from beaming sources. $\alpha_x \leq \alpha_r$ may be indicative of beaming whereas $\alpha_x > \alpha_r$ is the condition we expect from homogeneous synchrotron models.

5.2. Distinct spectral components

By this we mean a population of relativistic electrons which is distinct from that we measure in the radio/optical regime. The emitting volume could be quasi coincident with that of the known synchrotron component, or it could be embedded within the known volume. For synchrotron models, a small, flat spectrum component is required. In the case of the 25" knot in 3C 120, the current optical upper limits demand that $\alpha \leq 0.4$. A small region within the radio knot would be an efficient method to produce the observed X-rays in the sense that the total energy of such an entity would be very modest (Harris et al. 1998). As noted in sec 5.1, the spectral data so far available do not support this sort of scenario.

For the IC/CMB model without beaming, what is required is an excess population of electrons with γ in the range 500-2000. For bulk relativistic velocities, this energy range shifts to lower values since the peak of the CMB appears blue shifted to the jet.

5.3. Jet length and structure

The beaming model has untenable consequences for straight jets. In general, the angle, θ, between the jet axis and line of sight to the observer derived for jets such as 3C 273 are not very different from those found at VLBI scales, and this jet appears straight on the kpc scale. If the jet fluid moves in a straight line along the axis of the jet, then the physical length of the jet is the projected length divided by sin θ. In Table 2 we have listed these values which range up to a Mpc for 3C 273. Very few radio sources are directly observed (i.e. in the plane of the sky) to have such large physical sizes.

These excessive lengths can be avoided in at least two ways. We know that some jets bend (e.g. 3C 120). If the apparently straight jets (e.g. 3C 273) were to bend significantly in a plane normal to the plane of the sky, they would appear straight but the beaming required for a particular feature would not apply to the whole jet. The other possibility is that the jet fluid responsible for the observed radiation would not be constrained to move along the jet axis, but, for example, might follow a helical path (see e.g. Meier, Koida, and Uchida, 2001) around the axis as suggested by the HST images of 3C 273, or the emission regions might represent all or a portion of the flow being deflected toward the observer.

Whichever of these possibilities might be operative, it should work in conjunction with the requirement that the jet seen is the one approaching the observer.

5.4. Evidence for bulk relativistic velocities and cold jets

Are there reasonable expectations for kpc scale relativistic velocities aside from their utility in explaining X-ray emission? Bridle (1996) marshals considerable evidence for bulk relativistic velocities at least for the inner section of FRI jets, and all the way out to the terminal hotspots for FRII radio galaxies and quasars. Although representative values for such velocities are not presented, we infer Γ values of at least a few. Wardle & Aaron (1997), while agreeing that one-sidedness evidence supports relativistic velocities in jets, argue that the observed dispersion in the ratio of the flux density of the inner straight part of the jet (the feature expected to be most enhanced by beaming) to the flux density of the lobe (no beaming) is less than the expected dispersion for $\Gamma \approx 5$. Thus they conclude that the characteristic jet speed is $\beta \approx 0.85$ ($\Gamma \approx 2$) and that all jets decelerate between pc and kpc scales.

The consideration of large Γ values for kpc scale jets reminds us of the problem of energy transport. If electrons were to be a significant component of

the jet, they cannot escape the IC losses which increase as Γ^2. Since these losses go as γ^2, we may expect that only low energy electrons survive for long distances. Thus the energy must be transported by Poynting flux, protons, or cold electrons and positrons. If the latter, it might be possible to explain the relatively smooth X-ray emission such as that underlying the 3C 273 knots or the Pictor A inner jet, as IC beamed emission from essentially cold electrons which are characterized by $\Gamma \geq \gamma$. The brighter knots would then rely on the conventional shock acceleration and/or pair production to generate (in situ) the usual power law distribution of relativistic electrons with γ values of normal synchrotron sources.

5.5. Offsets between radio and X-ray brightness peaks

The synchrotron expectation is that lower frequency emission will persist further downstream since the higher energy electrons have shorter lifetimes. However, at the site of the shock, there should be strong emission at all frequencies (e.g. M87, knot A). In the beaming model, one way to accommodate a leading X-ray feature is to argue for the existence of a precursor shock which is incapable of producing electrons with $\gamma \geq 1000$.

5.6. Progression of brightnesses for multiple knot jets

In the optical, the 3C 273 jet has a series of well defined knots with comparable brightnesses and fluxes. However, at radio wavelengths, the knot intensities increase going out the jet and the situation is reversed for X-rays. This X-ray and radio behavior is mimicked in PKS1127. As a natural consequence, the parameters for the beaming model become less restrictive (smaller Γ, larger θ) as the distance from the core increases.

This sort of behavior is consistent with synchrotron models for which we might well expect that the properties of shocks which permit them to produce copious supplies of the highest energy electrons will diminish as we move out to larger distances.

5.7. Is overproduction a problem?

The beaming model means that the underlying synchrotron components are significantly less energetic than for the stationery synchrotron model. Typical luminosities drop from 10^{41} erg s^{-1} to values like 10^{38} erg s^{-1}. Such entities must be very common in jets, so might we expect to be overwhelmed with X-ray emission from excessive numbers of weak synchrotron emitters which happen to be moving towards us?

6. Conclusions

There is little doubt in our minds that thermal bremsstrahlung is not a major contributor to the X-ray emission from most of the jet features discussed in this paper. We find the arguments in favor of SSC emission from terminal hotspots of a few FRII radio galaxies to be convincing.

The failure of simple synchrotron models to fit the spectra of some features, together with the quasi-universality of one-sidedness almost demands the occurrence of relativistic bulk velocities. On the other hand, extreme values for the beaming parameters together with the excellent agreement of the X-ray spectra with the extrapolation of the radio-optical spectra for many features lend strong support to the synchrotron models.

Thus the leading contender for most of the X-ray jets appears to be a single or multiple spectral component synchrotron model augmented by a modest beaming with $\Gamma < 10$ to account for the one-sidedness of most of the recorded X-ray features. The IC/beaming hypothesis can consistently explain the emission from several jets, and the low required beaming factors for some sources as e.g. PKS 1127 make it probable that this emission component contributes substantially to the observed X-ray fluxes of at least some of the observed X-ray features. Higher redshifts and steeper radio spectra appear to favor beaming, while local sources with flatter radio spectra are probably dominated by synchrotron emission.

DEH thanks W. Tucker for extensive discussions during the early phases of this investigation, T. Kneiske for discussions on comparison of beaming formulations, and A. Bridle for discussing the radio aspects of jets. We also thank M. Hardcastle, M. Birkinshaw, and R. Sambruna for communicating results prior to publication and A. Siemiginowska and H. Marshall for sharing their proprietary data. M. Birkinshaw, D. Worrall, W. For-

man, F. Aharonian, and A. Marscher provided helpful suggestions for improving the manuscript and the anonymous referee supplied useful criticisms. HK thanks P. Coppi for discussions on AGN jets, and acknowledges support by NASA (NAS8-39073 and GO 0-1169X). The work at SAO was partially supported by NASA contract NAS8-39073.

A. Formulation of bulk relativistic beaming with equipartition fields

We first find the synchrotron parameters in the jet frame and then derive expressions for the IC emission. Then we obtain two expressions for the ratio of IC to synchrotron losses: one based on the observed data and one based on the energy densities of phtons and magnetic fields. Equating these two expressions provides the final beaming equation. We use cgs units throughout except where stated otherwise.

The basic relationships for the parameters which describe the bulk motion of the jet fluid are the jet velocity, $\beta_{\rm j} \equiv \frac{v}{c}$; the Lorentz factor, Γ; the angle of the fluid's velocity with respect to the line of sight of the observer, $\theta_{\rm j}$; and the Dopler beaming factor, δ.

$$\Gamma \equiv \frac{1}{\sqrt{1 - \beta^2}} \tag{A1}$$

$$\delta^{-1} = \Gamma(1 - \beta \, cos \, \theta) \tag{A2}$$

A.1. The synchrotron parameters in the jet frame

The required observables are:

- the size of the emitting volume
- α, the low frequency spectral index of the synchrotron spectrum.
- ν_1 and ν_2, the lower and upper limits of the synchrotron spectrum in the observer frame. NB: It may be necessary to decrease ν_1 to ≈ 1 MHz so as to include low γ electrons required for the beaming model.
- $S_{\rm o}$ at some $\nu_{\rm o}$, with $S_{\rm o}$ the flux density observed at the Earth, and $\nu_{\rm o}$ the frequency at the receiver corresponding to $S_{\rm o}$. This provides k_s, the amplitude of the observed synchrotron spectrum: $k_s = S_{\rm o} \, \nu_{\rm o}^{\alpha}$.
- The luminosity distance and redshift.

We then move to the jet frame. Frequencies convert as:

$$\nu' = \nu \, (1 + z)/\delta \tag{A3}$$

Assuming a knotty jet and neglecting complications arising from different pattern and jet plasma velocities, we find from the Lorentz invariant, S/ν^3 (see also eqs. C7 and C11 of Begelman, Blandford, & Rees 1984), the monochromatic luminosity per solid angle in the jet frame:

$$l'_{\Omega,\nu'} = \frac{k_s(obs) \; \nu'^{-\alpha} (1 + z)^{\alpha - 1} \; D_{\rm L}^2}{\delta^{3+\alpha}} \quad \text{erg cm}^{-2} \text{ s}^{-1} \text{ Hz}^{-1} \text{ str}^{-1} \tag{A4}$$

Here, $D_{\rm L}$ is the luminosity distance and $(1 + z)^{\alpha - 1}$ is the K-correction. This equation allows evaluation of $l'_{\Omega,\nu'}$ at any convenient frequency in the jet frame. Integrating over frequency and solid angle, the total luminosity becomes:

$$L'_s = \left[\frac{4\pi D_{\rm L}^2}{\delta^4}\right] \left[\frac{k_s \, (\nu_2^{1-\alpha} - \nu_1^{1-\alpha})}{(1 - \alpha)}\right] = \frac{L_s}{\delta^4} \quad \text{erg s}^{-1} \tag{A5}$$

The right term is the energy flux at the Earth, $4\pi \; D_{\rm L}^2$ computes the luminosity at the source, and δ^4 transforms into the jet frame.

To compute the equipartition magnetic field in the jet frame (e.g. eq. 7.12 of Pacholczyk, 1970):

$$B'_{\rm eq} = \left[\frac{18.85\, C_{12}\, (1+k)\, L'_s}{\phi V'}\right]^{2/7} \quad \text{Gauss} \tag{A6}$$

V' is the emitting volume; ϕ is the volume filling factor; and C_{12} is a Pacholczyk parameter which is a slowly varying function of α, ν'_1, and ν'_2 (e.g. C_{12}=5.7×10^6 for $\alpha = 0.8; \nu'_1 = 10^7; \nu'_2 = 10^{15}$). When the correct expression for C_{12} is used in eq. A6, it introduces an extra factor of $\delta^{0.5}$ to the numerator within square brackets, so that together with the explicit δ^4 from eq. A5 which appears in the denominator, the final dependency within the square brackets goes as $\delta^{-\frac{7}{2}}$ and hence:

$$B'_{\rm eq} = \frac{B(1)}{\delta} \tag{A7}$$

where B(1) is the equipartition field calculated for no beaming (δ=1).

A.2. Converting angles to the jet frame in order to calculate the IC emission

From manipulation of the basic equations (A1, A2):

$$\mu_{\rm j} \equiv \cos(\theta_{\rm j}) = \frac{\Gamma - 1/\delta}{\sqrt{\Gamma^2 - 1}} \tag{A8}$$

Since in the jet frame most of the CMB photons will come from the direction in which the jet plasma is moving and the scattered IC emission from a particular electron will be strongly beamed into the direction of the instantaneous velocity vector of the electron, the IC emission will not be isotropic in the jet frame. Take the angle between the l.o.s. to the observer and the jet axis as $\theta_{\rm j}$ and $\theta'_{\rm j}$ in the observer and jet frames, respectively. Likewise, $\mu_{\rm j}$ and $\mu'_{\rm j}$ are the corresponding cosines. Then:

$$\mu'_{\rm j} = \frac{\mu_{\rm j} - \beta_{\rm j}}{1 - \mu_{\rm j}\, \beta_{\rm j}} \tag{A9}$$

where $\beta_{\rm j}$ is the velocity of the jet (see e.g. Pacholczyk 1970, eq. 5.25). The inverse is also useful:

$$\mu_{\rm j} = \frac{\mu'_{\rm j} + \beta_{\rm j}}{1 + \mu'_{\rm j}\, \beta_{\rm j}} \tag{A10}$$

To calculate the power emitted by an electron traveling at an angle Θ' to the seed photon direction, we use $\Theta' \approx \theta'_{\rm j}$ and follow Rybicki & Lightman (1979, p. 199, see also Dermer et al. 1992) to get:

$$\frac{dE'}{dt} = c\, \sigma_T\, u'_{\rm CMB}\, \kappa \quad \text{erg s}^{-1} \tag{A11}$$

$$\kappa = \gamma'^2_{\rm e}(1 + \beta'_{\rm e}\, \mu'_{\rm j})^2 - (1 + \beta'_{\rm e}\, \mu'_{\rm j}) \tag{A12}$$

where $\sigma_{\rm T}$ is the Thomson cross section; E' is the energy of the electron; $u'_{\rm CMB}$ is the Doppler boosted energy density of the CMB; and $\gamma'_{\rm e}$, $\beta'_{\rm e}$ are the Lorentz factor and velocity of the electron in the jet frame.

The second term in eq.A12 will be negligible except when $\mu'_{\rm j}$ approaches minus one, which is the case for electrons moving directly away from the jet's velocity vector.

The energy density of the CMB (as seen by the jet moving with Γ):

$$u'_{\rm CMB} = 4 \times 10^{-13}\, (1+z)^4\, (4/3)\, (\Gamma^2 - 1/4) \quad \text{erg cm}^{-3} \tag{A13}$$

The peak frequency of the CMB (again, as seen by the jet)

$$\nu'_{\rm p} = 1.6 \times 10^{11}\,(1+z)\,\Gamma \quad {\rm Hz} \tag{A14}$$

In the jet frame, the mean energy of photons scattered in the direction $\theta'_{\rm j}$ will be:

$$< \varepsilon'_{\rm IC} >= \frac{dE'/dt'}{\left[c\,\sigma_{\rm T}\,n'_{\rm CMB}\,(1+\beta'_{\rm e}\,\mu'_{\rm j})\right]} \quad {\rm erg} \tag{A15}$$

$$= \frac{< \varepsilon'_{\rm p} > \kappa}{1+\beta'_{\rm e}\,\mu'_{\rm j}} \quad {\rm erg} \tag{A16}$$

$$=< \varepsilon'_{\rm p} > \left[\gamma'^2_{\rm e}(1+\beta'_{\rm e}\,\mu'_{\rm j})-1\right] \quad {\rm erg} \tag{A17}$$

where $< \varepsilon'_{\rm p} >$ is the mean energy of the photons before scattering: $1.6 \times 10^{11}(1+z)\Gamma$, and $n'_{\rm CMB}$ is the seed photon density in the jet frame, so that the denominator in Eq. (A15) is the (expected) number of scatterings per unit time for one electron.

A.3. The expression for the observed ratio of luminosities, R(obs)

We define R as the ratio of IC and synchrotron luminosities. Since both of these losses goes as the electron energy squared, all electrons will experience the same value of R.

For $\alpha = 1$, there is equal energy per decade and thus the integration band is not important so that the ratio of luminosities is equal to the ratio of amplitudes of the X-ray (IC) and radio (sync) spectra.

$$R(1) = \frac{L_{ic}}{L_{sync}} = \frac{k_x}{k_r} \tag{A18}$$

For $\alpha \neq 1.0$, to obtain L_{ic}/L_{sync} we change integration parameters from ν' to γ'. These conversions are found by using Eq. (A17) with $\beta'_{\rm e}$=1 and dropping the '-1':

$$\nu'_{\rm ic} = (1+\mu'_{\rm j})\,\gamma'^2_{\rm e}\,[1.6\,\times\,10^{11}\,(1+z)\,\Gamma] \quad {\rm Hz} \tag{A19}$$

(the last term is the peak frequency of the CMB in the jet frame)

$$\nu'_{sync} = 4.202\,\times\,10^6\,\gamma'^2_{\rm e}\,\times\,B' \quad {\rm Hz} \tag{A20}$$

Then most of the factors of eq. A5 including the integration itself, cancel and the remaining parameters are those resulting from the different conversions of ν to γ. After these manipulations, we find:

$$R(obs) = R(1)\left[\frac{3.808\,\times\,10^4\,(1+z)\,(1+\mu'_{\rm j})\,\Gamma}{B'_{\rm eq}}\right]^{1-\alpha} \tag{A21}$$

A.4. Evaluate R from ratio of energy densities

The ratio of the IC and synchrotron luminosities can be computed from the ratio of energy densities in photons and magnetic field. This provides an expression for the 'expected' value of R. In using eq.(A12), we have dropped the second term since it will normally be much smaller than the first term.

$$R(exp) \;=\; \frac{U'_{\rm CMB}}{u'(B'_{\rm eq})},= \;\frac{4\,\times\,10^{-13}\,(1+z)^4\,(1+\mu'_{\rm j})^2\,\left[\Gamma^2-(1/4)\right]}{B'^2_{\rm eq}/8\pi} \tag{A22}$$

where $U'_{\rm CMB}$ is the CMB energy density in the jet frame, modified by the deviation from the beamed emission power from that computed for an isotropic seed photon field.

A.5. The beaming equation

Equating the two expressions for R (Eqs. A21 and A22),

$$\Gamma^{\alpha+1} - \frac{\Gamma^{\alpha-1}}{4} \;=\; R(1)\,\frac{9.947\;\times\;10^{10}\,(3.808\;\times\;10^{4})^{1-\alpha}}{(1+z)^{3+\alpha}}\left[\frac{B'_{\rm eq}}{1+\mu'_{\rm j}}\right]^{\alpha+1} \tag{A23}$$

Thus with 4 parameters which depend on the observable data (α, z, B(1), and R(1)) we can solve eq. A23 numerically by finding the range of μ' and Γ pairs which satisfy the equation.

If we ignore the second Γ term and replace B$'$ with eq. A7, we obtain an approximate expression for the beaming parameters in terms of the observables (see fig. 2):

$$\Gamma\delta(1+\mu'_{\rm j}) = \frac{B(1)[10^{11}R(1)]^{\frac{1}{1+\alpha}}(3.808\;\times\;10^{4})^{\frac{1-\alpha}{1+\alpha}}}{(1+z)^{\frac{\alpha+3}{\alpha+1}}} \tag{A24}$$

B. Frequencies, electron energies, and halflives

Once we have the allowed values of $\theta_{\rm j}, \delta$, and Γ, we need to determine where the emission bands occur and which segments of the electron energy spectrum are responsible for the observed radiation.

To determine the IC emission frequency of electrons responsible for a particular synchrotron frequency:

$$\nu_{\rm ic}(obs) = \nu_s(obs)\,3.808\;\times\;10^4\,(1+\mu'_{\rm j})\,\Gamma(1+z)/B' \quad {\rm Hz} \tag{B1}$$

and the reverse:

$$\nu_s(obs) \;=\; \frac{\nu_{\rm ic}(obs)\,2.626\;\times10^{-5}\,B'}{\Gamma(1+z)(1+\mu'_{\rm j})} \quad {\rm Hz} \tag{B2}$$

To find the electron energy responsible for a particular synchrotron frequency, we use eqs A3, A7, and A20:

$$\gamma'^2_{\rm e} \;=\; \frac{2.380\times10^{-7}\,\nu_s(obs)\,(1+z)}{B'\,\delta} \tag{B3}$$

For the electron energy responsible for an IC frequency we use eqs A3 and A19:

$$\gamma'^2_{\rm e} \;=\; \frac{6.25\times10^{-12}\,\nu_{\rm ic}(obs)}{(1+\mu'_{\rm j})\delta\Gamma} \tag{B4}$$

For the halflives, we use the normal expression: $(dE/dt)\times\tau = E/2$. This results in:

$$\tau' \;=\; \frac{10^{13}}{\gamma'_{\rm e}\left\{1.016\,B'^2\;+\;10.398\,(1+z)^4(\Gamma^2-\frac{1}{4})\left[(1+\beta'_{\rm e}\mu'_{\rm j})^2-\frac{(1+\beta'_{\rm e}\mu'_{\rm j})}{\gamma'^2_{\rm e}}\right]\right\}} \tag{B5}$$

where B' is in μG and τ' is in years.

Making the usual approximations for quantities close to one, and since time intervals in the jet frame are observed at the Earth as:

$$\tau_{\rm o} = \tau'\,\frac{(1+z)}{\delta} \tag{B6}$$

an approximate expression for the observed halflife is:

$$\tau_{\rm o} \, = \, \frac{10^{13}\,(1+z)}{\gamma'_{\rm e}\,\delta\,\{B'^2 \, + \, 40\,(1+z)^4\Gamma^2\}} \quad {\rm yrs} \tag{B7}$$

C. References

Aharonian, F.A. 2001, MNRAS (in press) astro-ph/0106037

Begelman, M., Blandford, R., & Rees, M. 1984, Rev. Mod. Phys. 56, on page 340, Eqs. C7 and C11

Biretta, J.A., Stern, C.P., and Harris, D.E. 1991 A.J., 101, 1632 (M87)

Bodo, G., Ghisellini, G., & Trussoni, E. 1992, MNRAS, 255, 694-700

Böhringer, H. et al. 2001, A&A 365, L181-L187 (M87)

Bridle, A.H. 1996 ASP Conference Series 100, 383-394, "Energy Transport in Radio Galaxies", Hardee, Bridle, & Zensus, eds.

Brunetti, G., Cappi, M., Setti, G., Feretti, L., Harris, D.E. 2001, A&A 372, 755

Burbidge, G.R. 1956, ApJ 124, 416-429

Carilli, C.L., Perley, R.A., & Harris, D.E. 1994, MNRAS 270, 173-177 (Cyg A)

Celotti, A., Ghisellini, G., & Chiaberge, M. 2001 MNRAS 321, L1-5

Chartas, G. et al. 2000 ApJ 542, 655 (PKS0637)

Dermer, C.D, Schlickeiser R., Mastichiadis A. 1992, A&A, 256, L27

Ginzburg, V.L. and Syrovatskii, S.I. 1969 ARA&A 7, 375

Hardcastle, M.J., Birkinshaw, M. & Worrall, D.M. 2001a MNRAS (accepted; 3C 123 astro-ph/0101240)

Hardcastle, M.J., Birkinshaw, M. & Worrall, D.M. 2001b MNRAS (submitted; 3C 66B astro-ph/0106029)

Harris, D.E., Carilli, C.L. and Perley, R.A. 1994 Nature 367, 713 (CygA)

Harris, D.E., Leighly, K.M., and Leahy, J.P. 1998 ApJ 499, L149-L152 (3C390.3)

Harris, D.E., Hjorth, J., Sadun, A.C., Silverman, J.D. & Vestergaard, M. 1999 ApJ 518, 213-218 (3C120)

Harris et al. 2000 ApJ 530, L81 (3C295)

Kraft, R.P. et al. 2000 ApJ 531, L9-L12 (Cen A)

Mannheim, K., Krulls, W.M., and Biermann, P.L. 1991 Astron Astrophys 251, 723

Marshall, H. et al. 2001a ApJ 549, L167 (3C 273)

Marshall, H. et al. 2001b ApJ (submitted) (M87)

Meier, D.L., Koide, S., & Uchida, Y. 2001, Science 291, 84-92

Pacholczyk, A.G. 1970, "Radio Astrophysics" W. H. Freeman , San Francisco

Readhead, A.C.S. 1994 ApJ 426, 51-59

Rybicki, G.B. & Lightman, A.P. 1979, "Radiative Processes in Astrophysics" John Wiley & Sons, New York

Sambruna, R.M., Urry, C.M. Tavecchio, F., Maraschi, L., Scarpa, R., Chartas, G., & Muxlow, T. 2001 ApJ 549, L161 (3C 273)

Schreier, E.J., Gorenstein, P., & Feigelson, E.D. 1982, ApJ 261, 42

Siemiginowska, A.L. et al. 2001 (in preparation) (PKS1127-145)

Singal, A. K. 1986, A&A, 155, 242-246

Tavecchio, F., Maraschi, L., Sambruna, R.M., & Urry, C.M. 2000, ApJ 544, L23

Wardle, J.F.C., & Aaron, S.E. 1997, MNRAS 286, 425-435

Wilson, A.S., Young, A.J., and Shopbell, P.L. 2001a, ApJ 544, L27 (CygA)

Wilson, A.S., Young, A.J., & Shopbell, P.L. 2001b, ApJ 547, 740 (PicA)

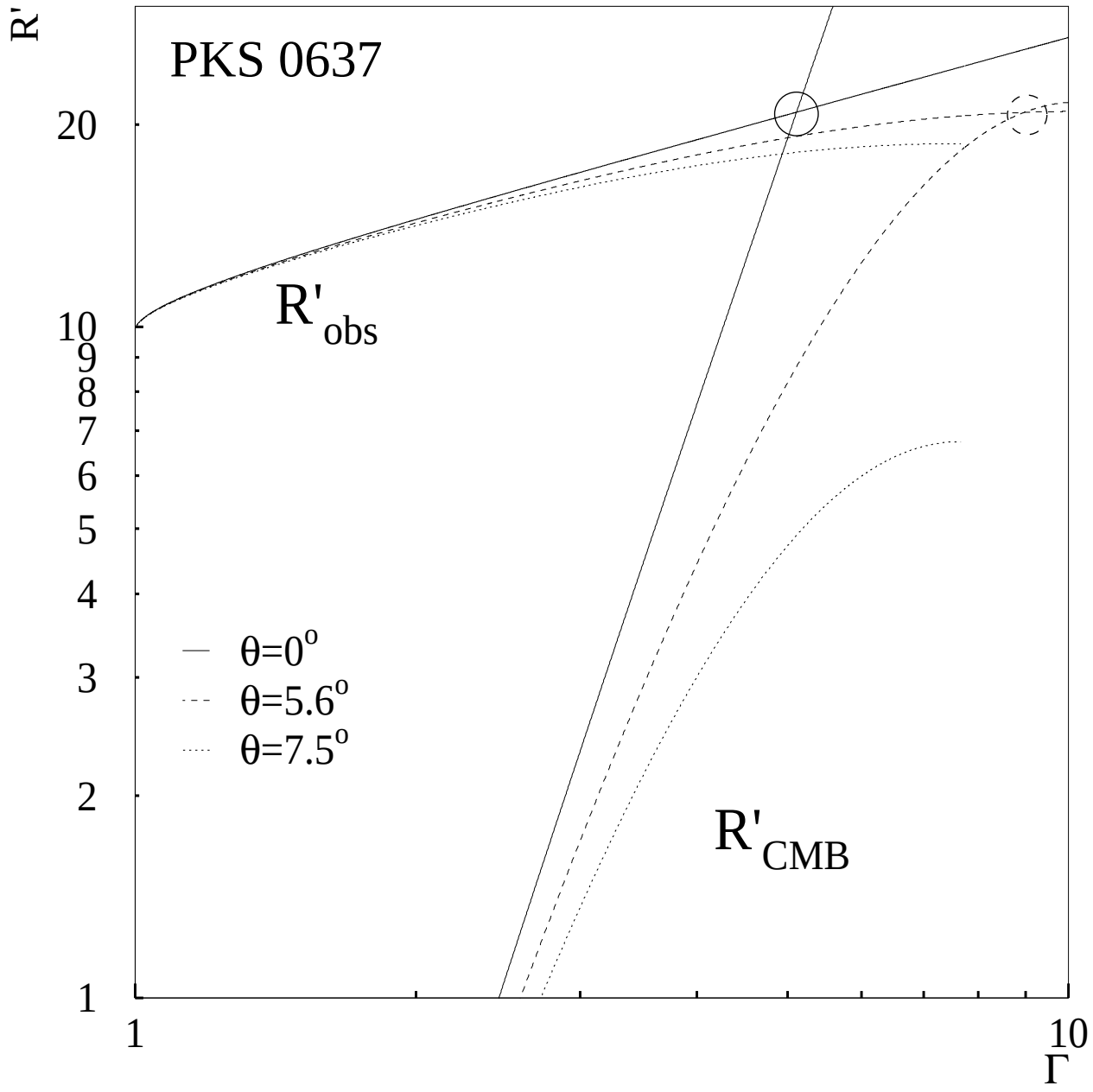

Fig. 1.— An illustration of the solutions for equations A21 and A22. The vertical axis is the ratio of IC to synchrotron losses in the jet frame and the horizontal axis is the Lorentz factor for the bulk velocity of the jet fluid. For PKS0637, the range of solutions run from θ =0 to 5.6°. For larger values of θ, there is no solution.

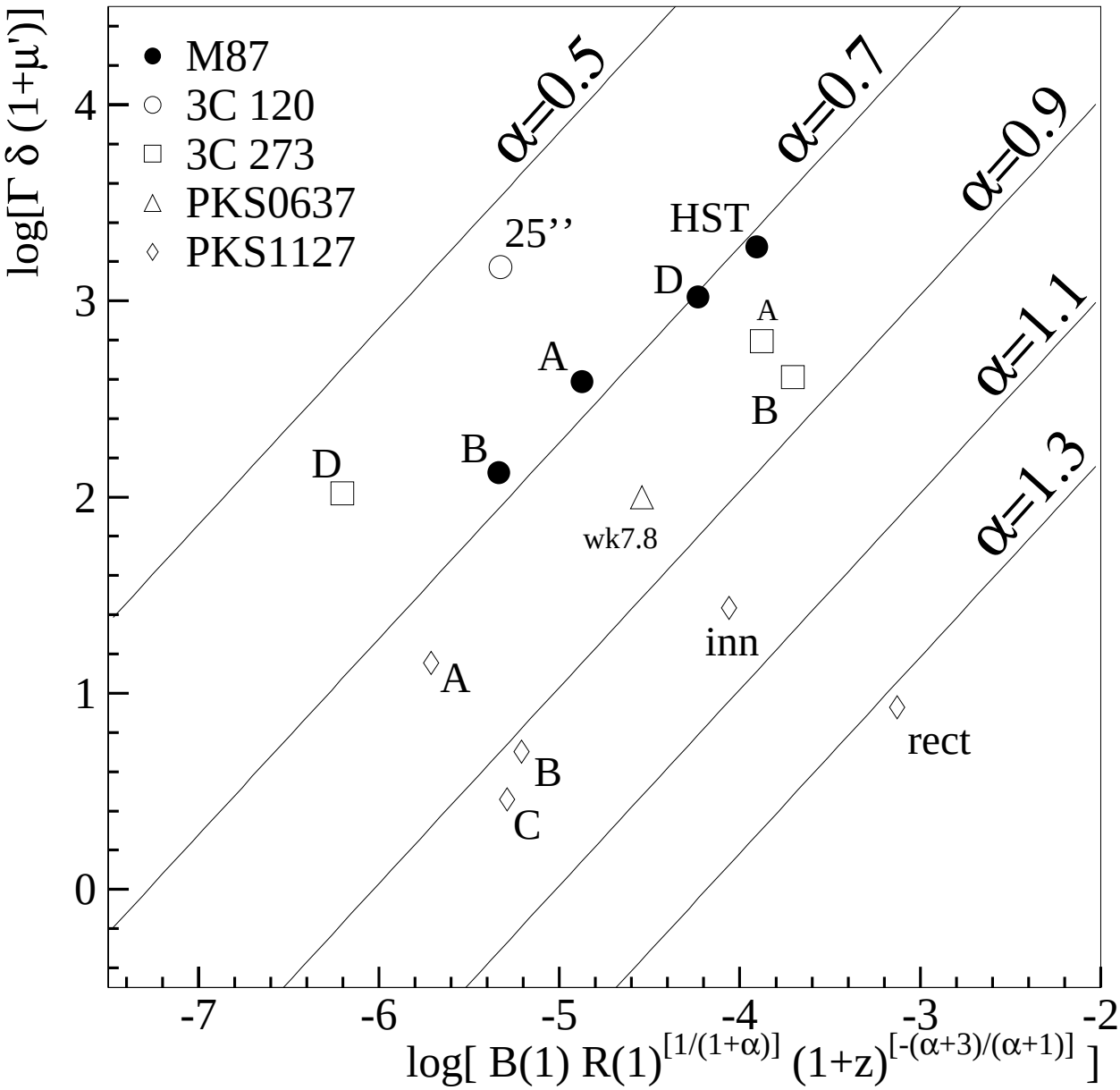

Fig. 2.— A graphic illustration of eq. A24. Since the second Γ term of eq. A23 has been dropped, the results shown here are indicative only. Solutions for several values of the spectral index are shown by the solid lines. The source data from Table 2 demonstrate that steeper spectra and higher redshifts require less beaming than do lower redshift, flatter spectra knots. Of the four 'observables' contributing to the X axis value, the equipartition field for no beaming, B(1) varies by a factor of 10, whereas R(1) varies by at least 9 orders of magnitude (mitigated here, of course, by the exponent which is usually less than unity).

Table 1: **2001 March list of radio sources with jet related X-ray emission**

Generic Name	RA J2000 hh mm	Dec J2000 dd mm	z	Dist. (H=50) (Mpc)	kpc/" (H=50)	Assoc. radio	Assoc. optical	PA w.r.t. core	Classification
3C 15	00 37	-01 09	0.0730	453	1.91	knots	knots	-30	nyc
3C 31	01 07	32 25	0.0167	101	0.47	jet	no	-20	nyc
3C 66B	02 23	43 00	0.0215	130	0.61	jet	jet	45	sync
3C 120	04 33	05 21	0.0330	201	0.91	knot	no	NW	beam?
3C 123	04 37	29 40	0.2177	1448	4.74	hs	no	110	SSC
PictorA	05 19	-45 46	0.0350	214	0.97	W hs	yes	-80	beam
PKS0521	05 25	-36 27	0.055	338	1.475	knots	yes	NW	nyc
PKS0637	06 35	-75 16	0.653	5197	9.22	knots	yes	-90	beam
PKS1127	11 30	-14 49	1.18	11257	11.48	yes	?	42	dis.morph.
3C 263	11 39	65 47	0.6563	5230	9.25	yes	no?	116	SSC
3C 273	12 29	02 02	0.1583	1025	3.70	knots	knots	190	sync,beam
NGC4261	12 19	05 49	0.00737	44	0.21	yes	no?	-90	nyc
M87	12 30	12 23	0.00427	16	0.077	knots	knots	-60	sync
Cen A	13 26	-42 49		3.5	0.017	?	?	70	dis.morph.
3C 295	14 11	52 13	0.45	3307	7.63	2hs	yes	-10	SSC
3C 371	18 06	69 49	0.051	314	1.38	yes	yes	WSW	sync
3C390.3	18 42	79 46	0.0561	346	1.50	hsB	hsB	-10	sync
Cyg A	19 59	40 44	0.0560	345	1.50	2hs	no	110/280	SSC

Notes and Comments
$q_\circ = 0$
References for individual sources as well as contact persons for unpublished data can be found at the XJET website: http://hea-www.harvard.edu/XJET/
In the classification column, 'nyc' means "not yet classified" (the data are unpublished) and 'dis.morph.' signifies "discrepant morphology".
Morphology: we generally use 'knot' to indicate a distinct brighter feature in a jet that continues past the feature and 'hotspot' either as the terminal bright enhancement at the end of an FRII jet, or as one of the multiple features associated with the termination of a jet. Normally 'knots' are found on the inner portion of FRI jets whereas 'hotspots' are mostly at the ends of FRII jets. However, we are not trying to impose distinct definitions, and infer no physical differences beyond these generalities.

Table 2: **Beaming parameters for selected jet features**

		INPUT PARAMETERS				BEAMING PARAMETERS			JET LENGTH		
Source	Knot	z	α	B(1) (μG)	R(1)	Γ δ	θ (deg)	R$'$	DfC (arcsec)	proj (kpc)	phys (kpc)
M87	HST-1	0.00267	0.71	272	0.264	40	1.2	551	1	0.08	4
	D	...	0.70	319	0.0568	33	1.8	123	3	0.23	7
	A	...	0.67	288	0.006	19	2.8	21	12	0.92	19
	B	...	0.67	248	0.0013	11	4.7	3	15	1.15	14
3C 120	25"	0.033	0.54	41	0.04	39	1.5	15764	25	23	869
3C 273	A1	0.158	0.79	172	1.09	25	2.3	246	13	48	1196
	B1	...	0.85	134	3.5573	20	2.8	166	17	62	1269
	D/H	...	0.57	221	0.00017	10	5.5	5	20	75	783
PKS0637	wk7.8	0.651	0.81	195	0.209	9.9	5.7	21	8	72	725
PKS1127	inner	1.187	1.0	144	8.426	5.2	11	8	1.5	17	89
	rect.	...	1.33	24	8.9E4	2.9	20	31	11	126	368
	A	...	0.76	13	0.667	3.7	15	287	12	138	533
	B	...	0.92	29	1.106	2.2	26	7	19	221	504
	C	...	0.94	29	0.754	1.5	32	3	28	321	606

		JET FRAME SYNCHROTRON PARAMETERS			HALFLIFE OBSERVED AT EARTH	
Source	knot	γ range (synchrotron)	γ range (0.3-8 keV)	B′(eq) (μG)	ν_s (max) (Hz)	$\tau[\nu_s(\mathrm{max})]$ (years)
M87	HST-1	30-9.4E5	12- 61	7	1E15	4.0
	D	22-8.7E5	20-107	10	1E15	7.7
	A	29-9.1E5	34-174	15	1E15	38.
	B	31-9.8E5	56-290	22	1E15	168.
3C 120	25”	77-2.4E4	17-89	1.1	1E11	153.
3C 273	A1	40-1.3E6	27-139	6.9	1E15	7.6
	B1	45-1.4E6	34-174	6.7	1E15	13.8
	D/H	35-1.1E6	67-348	22.	1E15	132.
PKS0637	wk7.8	45-1.4E6	68-351	20.	1E15	39.
PKS1127	inner	60-1.9E4	130- 669	28.	1E11	8348.
	rect.	147-4.6E4	232-1200	8.3	1E11	20300.
	A	200-6.3E4	182- 940	3.5	1E11	7195.
	B	134-4.2E4	306-1580	13.2	1E11	49500.
	C	134-4.2E4	449-2318	19.	1E11	138700.

NOTES

LENGTH: 'DfC' is distance from the core in arcsec, projected kpc, and de-projected kpc (= projected/sinθ) for no bending.

The gamma range for the radio (synchrotron spectrum) corresponds to the frequency range of 1 MHz to the value of ν_s(max) given in a later column. The synchrotron spectrum is assumed to extend down to 1 MHz in order to include the low energy electrons required for the beaming model.

ν_s(max) is the highest reliable synchrotron frequency: radio (E11 Hz) or optical (E15 Hz).

τ is the halflife for electrons that produce ν_s(max).

R′ is the ratio of IC to synchrotron losses in the jet frame.